RESIDUAL STRESS MINIMIZATION TO PREVENT PROCESS-INDUCED DAMAGES IN THICK-WALLED CFRP PIPES

Eui-Sup Shin and Hideki Sekine

Department of Aeronautics and Space Engineering, Tohoku University
Aramaki-aza-aoba 01, Aoba-ku, Sendai, 980-8579, Japan

SUMMARY: During the curing process of thick-walled multi-layered CFRP pipes, thermally induced stresses and deformations may cause various damages in the pipes, which naturally affect the ultimate structural performance. In this paper, an optimum design problem for the multi-layered CFRP pipes is formulated by minimizing the process-induced residual stresses under some constraints of structural stiffnesses. The analytic solutions of the residual stresses are obtained based on quasi-static thermoelasticity and Hashin's failure criteria are used for the formation of a strength-based objective function. The numerical results of optimization show that, in the case of cross-ply pipes, the residual stresses can be reduced to a certain level by controlling ply thicknesses. Matrix cracking is the primary damage mode in the thick-walled pipes because the transverse residual stress is relatively large. For angle-ply pipes, it is possible to further suppress the residual stresses by adjusting ply angles. The effects of wall thickness and axial pre-tension on the optimum solutions are also investigated.

KEYWORDS: CFRP pipe, process-induced residual stress, optimum design, cross-ply, angle-ply, damage, wall thickness, pre-tension

INTRODUCTION

Anisotropic composite laminates can be effectively designed and tailored for lightweight structures owing to their excellent specific material properties. The multi-layered thick-walled pipes are one of promising structures, suitable for aerospace applications such as landing gear cylinders, space station trusses, etc. However, it has been pointed out that the tubular structure made of CFRP (carbon fiber-reinforced polymer) is susceptible to thermally induced residual stresses upon cooling in the curing process [1-5]. Several factors affect the formation of residual stresses, such as chemical shrinkage strain due to polymer crosslinking, thermal property mismatch, overall anisotropy of composites, and geometric characteristics of pipes. There may be significant process-induced damages, especially in the case of thick-walled CFRP pipes, resulting in a drop of stiffness and strength of the structure [6]. Therefore, the residual stresses developed during fabrication processes generally have great influence on the ultimate structural performance.

In this paper, special attention is given to the analysis and optimum design of filament-wound composite pipes to reduce the process-induced residual stresses under some requirements of structural performance. An analytic model based on quasi-static thermoelasticity is used for the calculation of the residual stresses for thick-walled multi-layered pipes [5]. In addition, the Hashin's theory [7] is adopted to quantify the risk of probable damages, i.e., fiber breakage, matrix cracking and delamination. Thus, the optimum configurations of ply thicknesses and angles in multi-layered CFRP pipes can be obtained, which will prevent the process-induced damages owing to residual stresses during the curing process. Several representative results of numerical optimization are finally presented, considering the effects of stacking sequence, wall thickness and axial pre-tension on the optimum solutions.

RESIDUAL STRESSES IN THICK-WALLED PIPES

Analytic Solution of Process-Induced Residual Stresses

As shown in Fig. 1, the wall of a long circular pipe is made of n plies with the inner radius r_0, the outer radius r_n, the wall thickness h, the ply thickness t_i and the ply angle ϕ_i. In each ply, principal material coordinates are defined by rotating the cylindrical coordinates about the r axis. Since the portion far from the ends of the pipe is of interest, under the assumptions of axisymmetry and generalized plane strain, displacements of the ith ply take the following form:

$$u_x^{(i)} = Cx, \quad u_\theta^{(i)} = Dxr, \quad u_r^{(i)} = u_r^{(i)}(r) \tag{1}$$

where C and D are arbitrary constants, free of the plies. The cylindrical pipe may undergo a thermally induced twist. The unidirectional CFRP composite is assumed transversely isotropic. Thus, the stress-displacement relations are expressed in the cylindrical coordinates as follows:

$$\sigma_x^{(i)}(r) = \overline{Q}_{11}^{(i)}C + \overline{Q}_{12}^{(i)}\frac{u_r^{(i)}(r)}{r} + \overline{Q}_{13}^{(i)}\frac{du_r^{(i)}(r)}{dr} + \overline{Q}_{16}^{(i)}Dr - S_x^{(i)} + \sigma_o^{(i)} \tag{2a}$$

$$\sigma_\theta^{(i)}(r) = \overline{Q}_{12}^{(i)}C + \overline{Q}_{22}^{(i)}\frac{u_r^{(i)}(r)}{r} + \overline{Q}_{23}^{(i)}\frac{du_r^{(i)}(r)}{dr} + \overline{Q}_{26}^{(i)}Dr - S_\theta^{(i)} \tag{2b}$$

$$\sigma_r^{(i)}(r) = \overline{Q}_{13}^{(i)}C + \overline{Q}_{23}^{(i)}\frac{u_r^{(i)}(r)}{r} + \overline{Q}_{33}^{(i)}\frac{du_r^{(i)}(r)}{dr} + \overline{Q}_{36}^{(i)}Dr - S_r^{(i)} \tag{2c}$$

$$\tau_{x\theta}^{(i)}(r) = \overline{Q}_{16}^{(i)}C + \overline{Q}_{26}^{(i)}\frac{u_r^{(i)}(r)}{r} + \overline{Q}_{36}^{(i)}\frac{du_r^{(i)}(r)}{dr} + \overline{Q}_{66}^{(i)}Dr - S_{x\theta}^{(i)} \tag{2d}$$

$$S_x^{(i)} = \overline{Q}_{11}^{(i)}\varepsilon_x^{T(i)} + \overline{Q}_{12}^{(i)}\varepsilon_\theta^{T(i)} + \overline{Q}_{13}^{(i)}\varepsilon_r^{T(i)} + \overline{Q}_{16}^{(i)}\gamma_{x\theta}^{T(i)} \tag{3a}$$

$$S_\theta^{(i)} = \overline{Q}_{12}^{(i)}\varepsilon_x^{T(i)} + \overline{Q}_{22}^{(i)}\varepsilon_\theta^{T(i)} + \overline{Q}_{23}^{(i)}\varepsilon_r^{T(i)} + \overline{Q}_{26}^{(i)}\gamma_{x\theta}^{T(i)} \tag{3b}$$

$$S_r^{(i)} = \overline{Q}_{13}^{(i)}\varepsilon_x^{T(i)} + \overline{Q}_{23}^{(i)}\varepsilon_\theta^{T(i)} + \overline{Q}_{33}^{(i)}\varepsilon_r^{T(i)} + \overline{Q}_{36}^{(i)}\gamma_{x\theta}^{T(i)} \tag{3c}$$

$$S_r^{(i)} = \overline{Q}_{13}^{(i)}\varepsilon_x^{T(i)} + \overline{Q}_{23}^{(i)}\varepsilon_\theta^{T(i)} + \overline{Q}_{33}^{(i)}\varepsilon_r^{T(i)} + \overline{Q}_{36}^{(i)}\gamma_{x\theta}^{T(i)} \tag{3d}$$

$$\varepsilon_x^{T(i)} = \int_{T_c}^{T}\alpha_x^{(i)}dT + \varepsilon_x^{C(i)}, \; \varepsilon_\theta^{T(i)} = \int_{T_c}^{T}\alpha_\theta^{(i)}dT + \varepsilon_\theta^{C(i)} \tag{4a,b}$$

$$\varepsilon_\theta^{T(i)} = \int_{T_c}^{T}\alpha_\theta^{(i)}dT + \varepsilon_\theta^{C(i)}, \; \gamma_{x\theta}^{T(i)} = \int_{T_c}^{T}\alpha_{x\theta}^{(i)}dT + \gamma_{x\theta}^{C(i)} \tag{4c,d}$$

where $\overline{Q}$ is the transformed stiffness coefficient, ε^T the process-induced strain, α the coefficient of thermal expansion, and ε^C the chemical shrinkage strain. The axial pre-tension,

$\sigma_o = E_1\varepsilon_o$, can be applied in 0° plies, indicating that the 0° plies are wrapped and stacked under a pre-stretched condition in the longitudinal fiber direction.
The analytical solution of the radial displacement can be derived by considering the equations of equilibrium with appropriate boundary conditions as

$$u_r^{(i)}(r) = C_1^{(i)} r^{k^{(i)}} + C_2^{(i)} r^{-k^{(i)}} + \left(m^{(i)} C + f^{(i)}\right) r + l^{(i)} D r^2 \tag{5}$$

$$k^{(i)} = \sqrt{\frac{\overline{Q}_{22}^{(i)}}{\overline{Q}_{33}^{(i)}}},\ m^{(i)} = -\frac{\overline{Q}_{12}^{(i)} - \overline{Q}_{13}^{(i)}}{\overline{Q}_{22}^{(i)} - \overline{Q}_{33}^{(i)}},\ f^{(i)} = \frac{S_r^{(i)} - S_\theta^{(i)}}{\overline{Q}_{22}^{(i)} - \overline{Q}_{33}^{(i)}},\ l^{(i)} = -\frac{\overline{Q}_{26}^{(i)} - 2\overline{Q}_{36}^{(i)}}{\overline{Q}_{22}^{(i)} - 4\overline{Q}_{33}^{(i)}} \tag{6}$$

Through a coordinate transformation, the residual stresses σ_1, σ_2, σ_3 and τ_{12} in the principal material coordinates are also calculated.

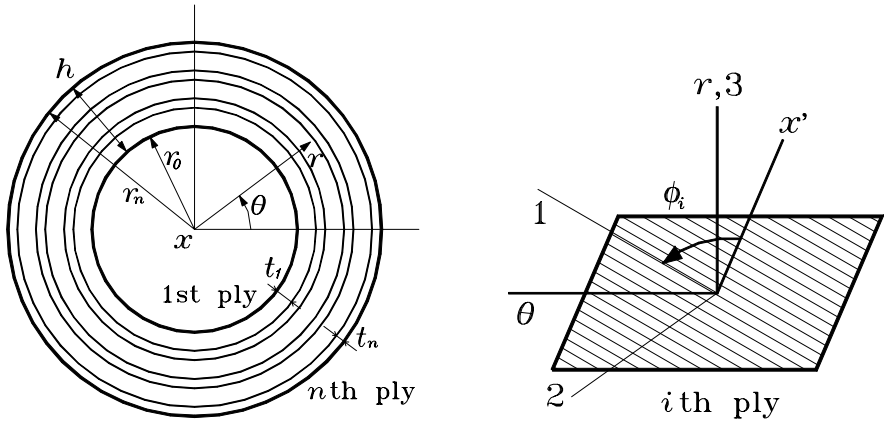

Fig. 1: Cross section of a multi-layered pipe and coordinate systems

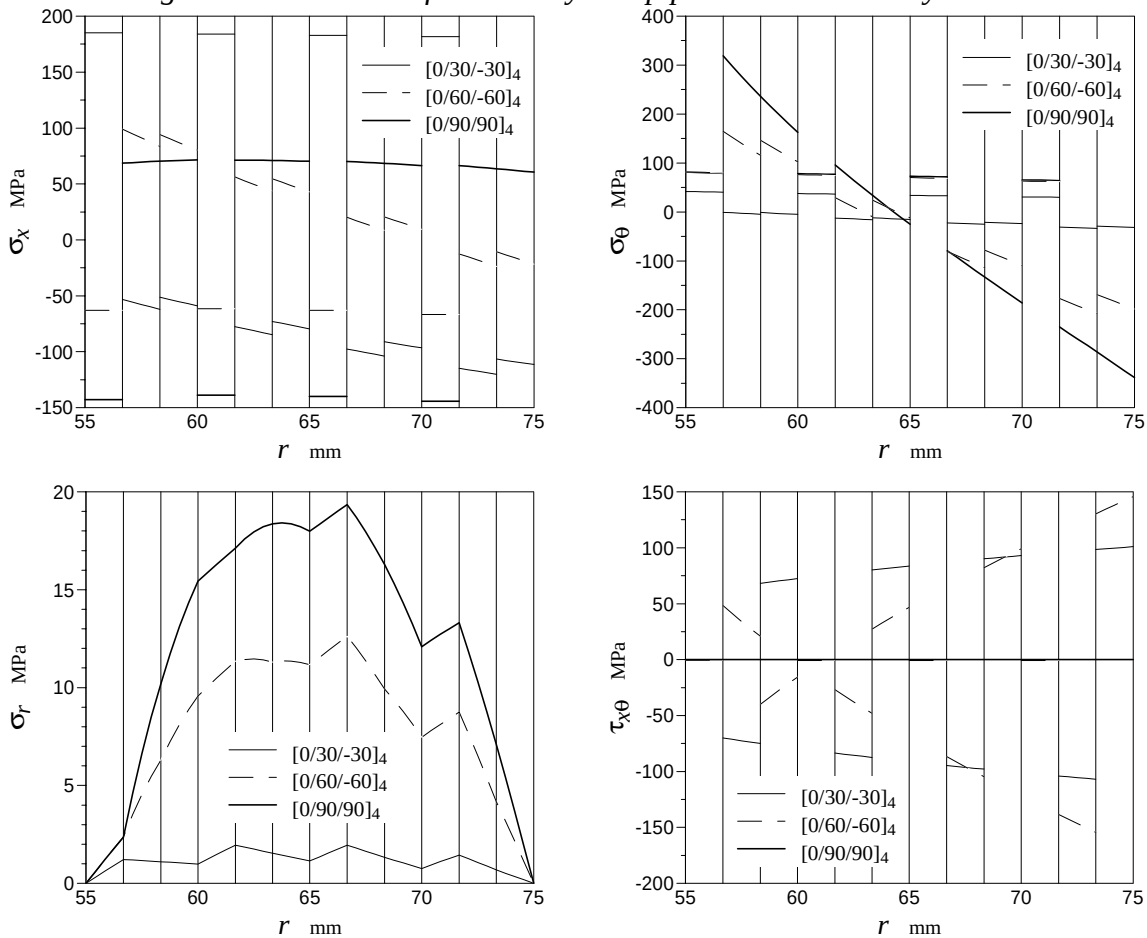

Fig. 2: Distributions of residual stresses in $[0/\phi/-\phi]_4$ pipes (r_n = 75 mm, h = 20 mm)

Typical Solutions on Residual Stresses for $[0/\phi/-\phi]_4$ Pipes

Fig. 2 shows the typical distributions of residual stresses through the thickness of the sample $[0/\phi/-\phi]_4$ pipes. The material properties of CFRP composite materials are used: $E_1 = 248$ GPa, $E_2 = 8.32$ GPa, $\nu_{12} = 0.326$, $\nu_{23} = 0.350$, $G_{12} = 3.08$ GPa, $\varepsilon_1^T = -2.52\text{x}10^{-5}$ and $\varepsilon_2^T = -8.43\text{x}10^{-3}$, where the curing temperature is supposed to be 150°C and the room temperature is 25°C. Note that the process-induced strain due to thermal expansion and chemical shrinkage is very smaller in the longitudinal fiber direction (1-axis) than in the transverse direction (2-axis) or in the through-the-thickness direction (3-axis).

As shown in Fig. 2, the patterns of the residual stresses in the CFRP pipes are quite different depending on the ply angle ϕ. The tensile axial stress σ_x is developed in 90° plies for $[0/90/90]_4$ pipe. Since there is no axial reinforcement in the 90° plies, it seems that the transverse stress σ_2 is large enough to initiate and propagate matrix cracking. The circumferential stress σ_θ is also tensile in all 0° plies. Although the circumferential stress in the 90° plies reaches about ±300 MPa, it acts in the longitudinal direction and well below the longitudinal strength of the CFRP composites. On the other hand, the radial stress σ_r is relatively small, compared to the other stresses. However, it must be noticed that the peak radial stress is tensile at interfaces between the plies. Owing to the low interlaminar strength of the usual laminated composites, the tensile radial stress may cause delamination damages. The shear stress $\tau_{x\theta}$ is always zeroed in the cross-ply pipe because there is no shear coupling in the constitutive relations.

FORMULATION OF OPTIMUM DESIGN PROBLEMS

Minimization of Failure Indices with Stiffness Constraints

A design problem is now formulated to search the optimum configurations, i.e., ply thicknesses and ply angles of thick-walled CFRP pipes that minimize the process-induced residual stresses in a strength-based sense. As an objective function, three maximum failure indices F_1, F_2 and F_3 (fiber breakage, matrix cracking and delamination, respectively) based upon Hashin's failure criteria [7] is considered as follows:

$$F = \max\left(F_{1\max}, F_{2\max}, F_{3\max}\right) \tag{7}$$

$$F_{1\max} = \max_{r_o \le r \le r_n} F_1(r) = \max_{r_o \le r \le r_n} \frac{|\sigma_1(r)|}{\sigma_{s1}} \tag{8a}$$

$$F_{2\max} = \max_{r_o \le r \le r_n} F_2(r) = \max_{r_o \le r \le r_n} \sqrt{\left(\frac{\sigma_2(r)+\sigma_3(r)}{\sigma_{s2}}\right)^2 + \frac{\tau_{12}^2(r) - \sigma_2(r)\sigma_3(r)}{\sigma_{s6}^2}} \tag{8b}$$

$$F_{3\max} = \max_{r_o \le r \le r_n} F_3(r) = \max_{r_o \le r \le r_n} \frac{\sigma_3(r)}{\sigma_{s3}} \tag{8c}$$

where σ_{s1}, σ_{s2}, σ_{s3} and σ_{s6} denote the longitudinal, transverse, interlaminar and shear strengths, respectively. For all numerical runs, the following strengths for CFRP composites are used: σ_{s1} = 1,320 MPa, $\sigma_{s2} = \sigma_{s3}$ = 56.1 MPa and σ_{s6} = 84.0 MPa. Although the current formulation is based upon the Hashin's theory, any other failure criteria such as maximum stress theory and Tsai-Wu theory may be applied to explicitly construct the form of the objective function.

In regard to the structural constraints of CFRP pipes, the global bending stiffness, transversely compressive stiffness and torsional stiffness must not be less than the respective lower limits.

$$G_1(X) = 1 - \frac{I_G(X)}{I_{G\,\min}} \le 0,\;\; G_2(X) = 1 - \frac{I_L(X)}{I_{L\,\min}} \le 0,\;\; G_3(X) = 1 - \frac{I_T(X)}{I_{T\,\min}} \le 0 \tag{9}$$

$$I_G = \frac{\pi}{4}\sum_{k=1}^{n} \overline{Q}_{11}^{(k)}\left(r_k^4 - r_{k-1}^4\right) \tag{10}$$

$$I_L = \frac{1}{3}\sum_{k=1}^{n} \overline{Q}_{22}^{(k)}\left[\left(r_k - r_c\right)^3 - \left(r_{k-1} - r_c\right)^3\right],\;\; r_c = \sum_{k=1}^{n} \overline{Q}_{22}^{(k)}\left(r_k^2 - r_{k-1}^2\right) \Big/ 2\sum_{k=1}^{n} \overline{Q}_{22}^{(k)}\left(r_k - r_{k-1}\right) \tag{11}$$

$$I_T = \frac{\pi}{2}\sum_{k=1}^{n} \overline{Q}_{66}^{(k)}\left(r_k^4 - r_{k-1}^4\right) \tag{12}$$

The augmented Lagrange multiplier method, combined with the BFGS variable metric method, is used as numerical optimization algorithm. In the current optimization, there really exist local solutions; that is, an objective function may not always converge to the same value, depending upon initial design variables. Therefore, to guarantee a reliable global optimum, the present calculation is carried out with sufficient variations in the initial design variables.

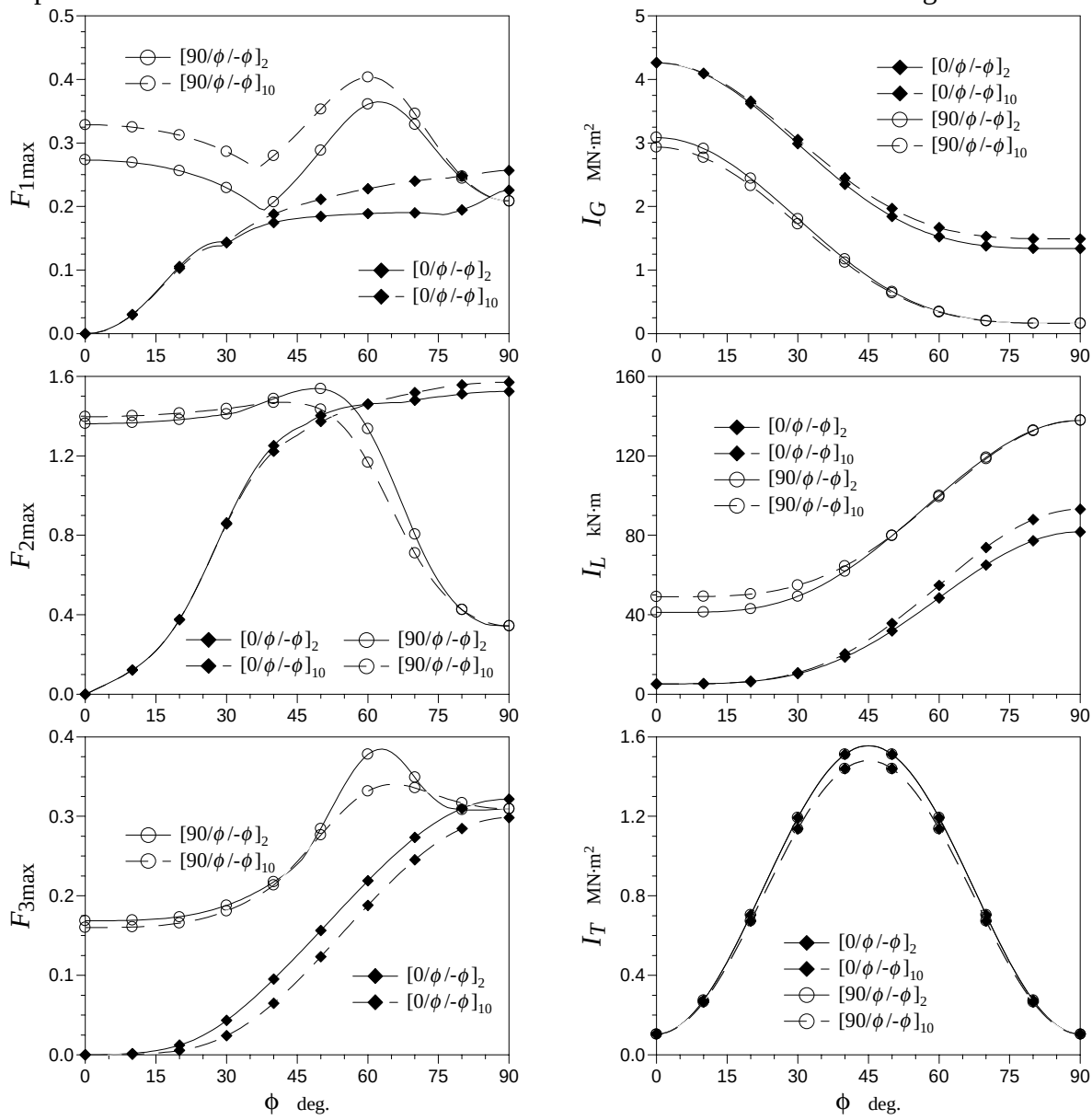

Fig. 3: Influence of ply angles on failure indices and structural stiffnesses

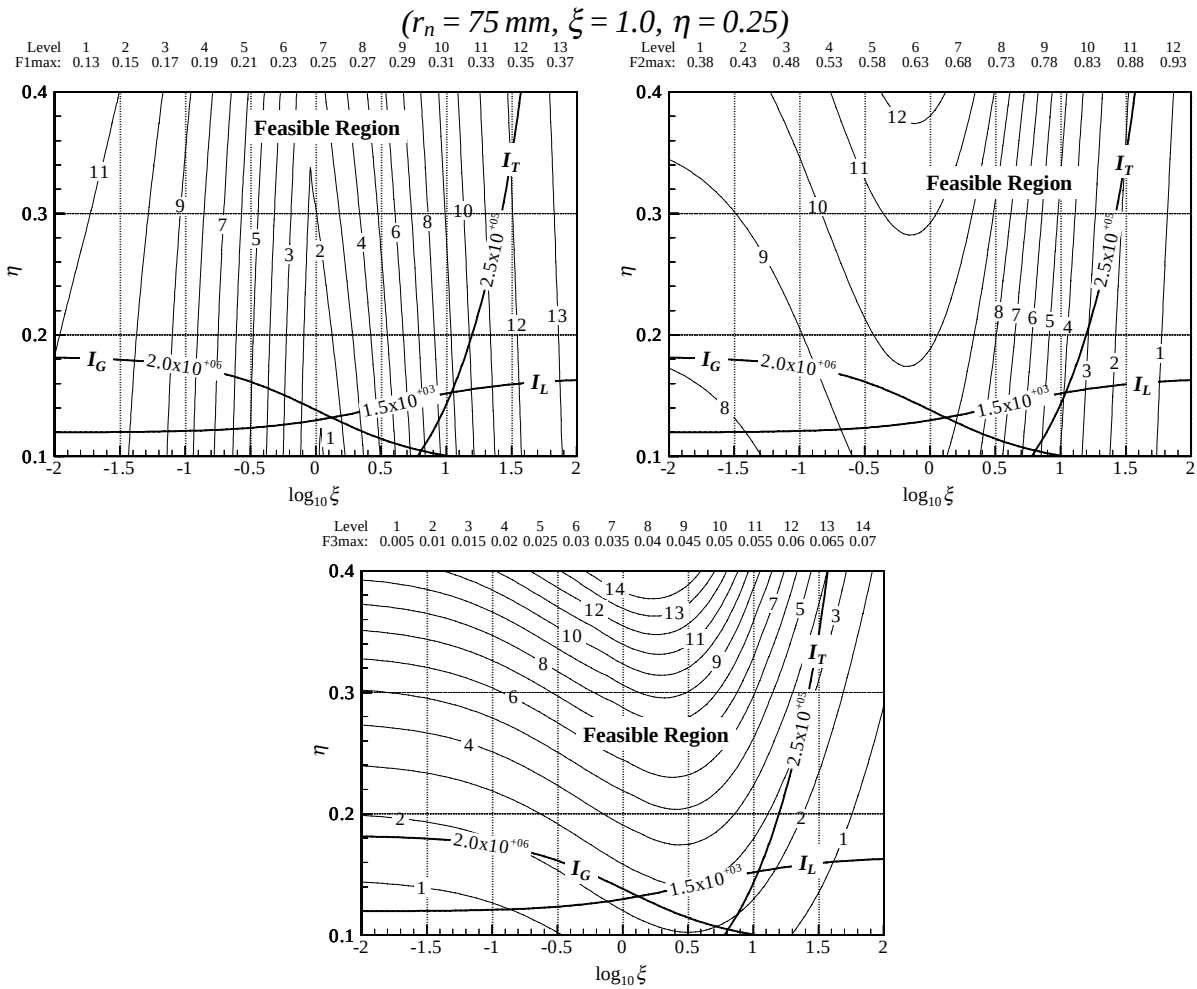

Fig. 4: Contours of failure indices in $\log_{10}\xi$-η space for $[0/30/-30]_4$ pipes (r_n = 75 mm)

Parametric Study for $[0/\phi/-\phi]_m$ and $[90/\phi/-\phi]_m$ Pipes

A parametric study is conducted as a prerequisite step for the optimum design of thick-walled CFRP pipes. The stacking sequences of the pipes are $[0/\phi/-\phi]_m$ and $[90/\phi/-\phi]_m$. Two design parameters are introduced representing the dimension and composition of the pipes as follows:

$$\xi = \frac{t_1}{t_2} = \frac{t_1}{t_3} = \cdots = \frac{t_{3m-2}}{t_{3m-1}} = \frac{t_{3m-2}}{t_{3m}}, \quad \eta = \frac{h}{r_n} = \frac{r_n - r_0}{r_n} \tag{13}$$

where the parameter ξ denotes a ratio of 0° or 90° ply thickness to ϕ or $-\phi$ ply thickness. The parameter η is a ratio of the wall thickness h to the outer radius r_n.

Fig. 3 shows the influence of ply orientations on failure indices and structural stiffnesses. On the whole, the results for $[0/\phi/-\phi]_m$ pipes are better than those for $[90/\phi/-\phi]_m$ pipes. The effect of the ply number $3m$ seems not serious. Note that all cross-ply pipes ($\phi = 0^o$ or 90°) have very small torsional rigidity. In Fig. 4, the contour lines of $F_{1\max}$, $F_{2\max}$ and $F_{3\max}$ are plotted in a $\log_{10}\xi-\eta$ space for $[0/30/-30]_4$ pipes. As expected, the respective maxima vary widely with the design parameters. It is significant that $F_{1\max}$ for fiber breakage mode increases in the region of high ξ, while $F_{2\max}$ for matrix cracking mode decreases in that region. In addition, the value of $F_{3\max}$ for delamination mode remains low in the whole region. Three thick solid lines represent bounds for the bending stiffness I_G = 2.0 MN·m^2, the transversely compressive

stiffness I_L = 1.5 kN·m and the torsional stiffness I_T = 0.25 MN·m^2, respectively. It is seen that, by selecting the parameters ξ and η appropriately, the failure indices can be reduced considerably.

OPTIMIZATION RESULTS AND DISCUSSION

Case of Cross-Ply CFRP Pipes

The optimization results for two types of cross-ply CFRP pipes are listed in Table 1. The pipes have an outer radius of 75 mm and a wall thickness of 18.75 mm. The design variables are ply thicknesses, which must be not be less than the allowable limit $t_{\min}$ = 0.1 mm. The lower limits of structural stiffnesses are prescribed as $I_{G\min}$ = 1.0 MN·m^2 and $I_{L\min}$ = 20 kN·m. In the case of C1, the critical index $F_{2\max}$ is minimized to 1.108 under the active constraint G_2. $F_{1\max}$ has also a relatively large value of 0.856. The difference between the C1 and C2 results is negligible.

The optimum ply thicknesses for the respective problems are shown in Fig. 5. It is found that only the middle 0° ply has large thickness and the thicknesses of the other plies are equal or near to the lower limit $t_{\min}$. Fig. 5 also depicts the distributions of three failure indices in the optimized cross-ply pipes. Because F_2 is high in 90° plies, the matrix cracking is probably the most dangerous damage. The torsional stiffness of these pipes is very small, I_T = 0.105 MN·m^2.

Table 1: Optimization results for cross-ply CFRP pipes (r_n = 75 mm, η = 0.25)

Cross-Ply	**Minimize *F***		Cross-Ply	**Minimize *F***	
C1	$F_{1\max}$	0.856	**C2**	$F_{1\max}$	0.858
[0°/90°/…/0°/90°]	$F_{2\max}$	**1.108**	[90°/0°/…/90°/0°]	$F_{2\max}$	**1.105**
(t_1/t_2/…/t_9/t_{10})	$F_{3\max}$	0.077	(t_1/t_2/…/t_9/t_{10})	$F_{3\max}$	0.075
constraint: G_1,G_2	G_2 active		constraint: G_1,G_2	G_2 active	

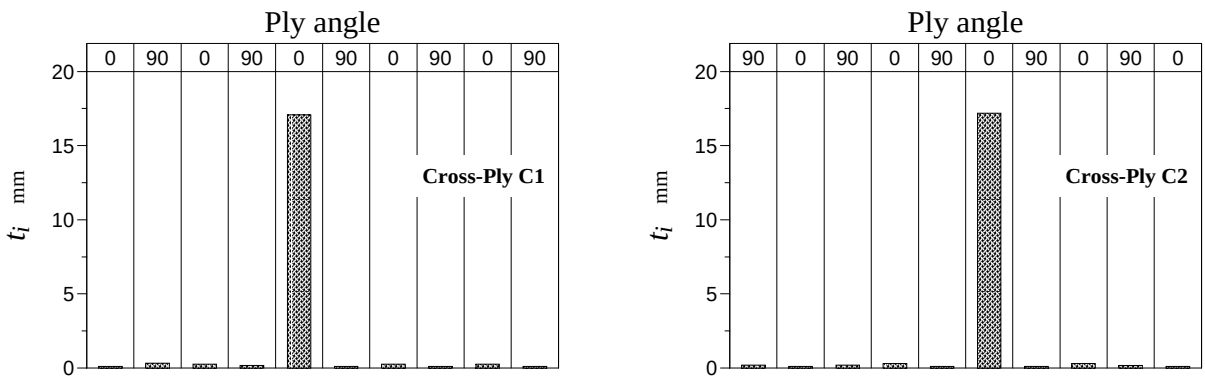

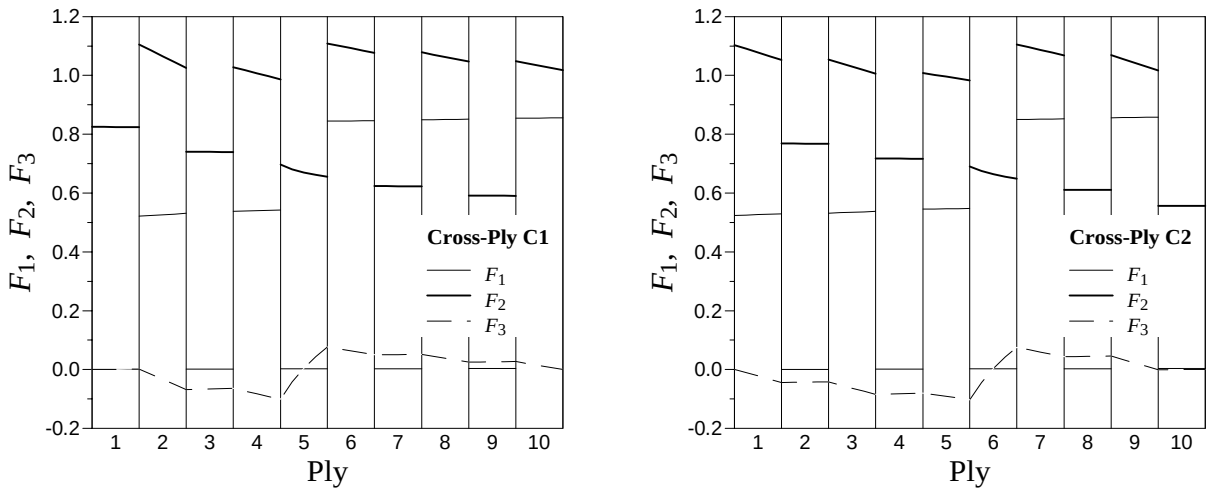

Fig. 5: Distributions of failure indices in optimized cross-ply pipes (r_n = 75 mm, η = 0.25)

Case of Angle-Ply CFRP Pipes

Next, the results of optimum design for angle-ply CFRP pipes are summarized in Table 2. The ply angles as well as the ply thicknesses are used as a set of design variables. The lower limit of torsional stiffness is now introduced as $I_{T\min} = 0.5$ MN·m^2. The optimum solutions for angle-ply pipes are somewhat improved in comparison with those for cross-ply pipes. In the case of A1, when the critical index $F_{2\max}$ is minimized to 0.961, the other indices $F_{1\max}$ and $F_{3\max}$ also become considerably low. Moreover, the constraint G_3 is not activated, implying the torsional stiffness of the optimized A1 pipe is large, I_T = 1.76 MN·m^2. However, the number of plies has minor influence on the optimized results for the angle-ply CFRP pipes. The reason is that the upper bounds of residual stresses developed in the pipes are affected by one or two key plies.

Corresponding to the above cases, the optimum ply thicknesses and angles are shown in Fig. 6. For example, the ply angles for A2 case range from 29.3^o to 40.8^o. Fig. 6 also represents the optimized distributions of failure indices in the angle-ply pipes. The index F_2 is significant over the entire plies. On the other hand, there is little risk of fiber breakage and delamination.

Table 2: Optimization results for angle-ply CFRP pipes (r_n = 75 mm, η = 0.25)

Angle-Ply	**Minimize *F***		Angle-Ply	**Minimize *F***	
A1	$F_{1\max}$	0.210	**A2**	$F_{1\max}$	0.254
$[\phi_1/-\phi_1/\ldots/\phi_3/-\phi_3]$	$F_{2\max}$	**0.961**	$[\phi_1/-\phi_1/\ldots/\phi_5/-\phi_5]$	$F_{2\max}$	**0.952**
$(t_1/t_1/\ldots/t_3/t_3)$	$F_{3\max}$	0.068	$(t_1/t_1/\ldots/t_5/t_5)$	$F_{3\max}$	0.068
constraint: G_1,G_2,G_3	G_2 active		constraint: G_1,G_2,G_3	G_2 active	

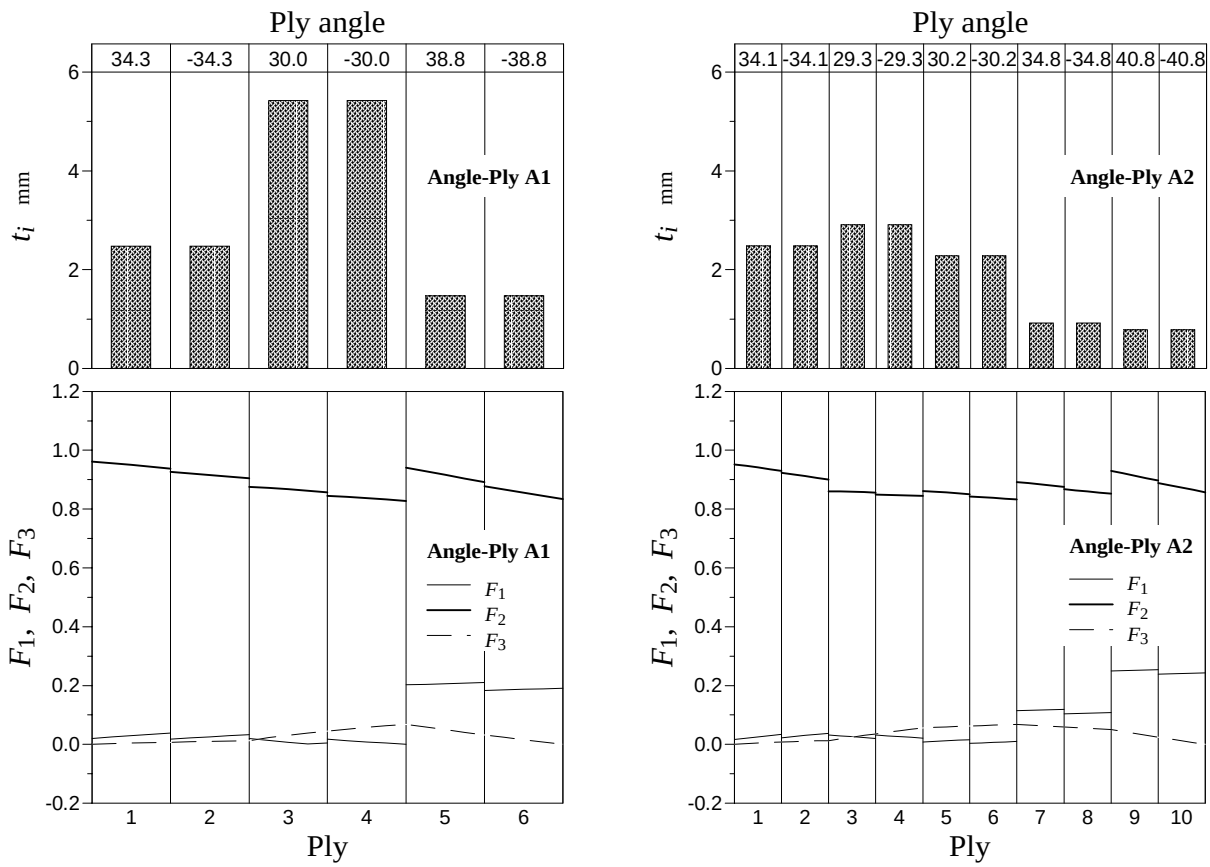

Fig. 6: Distributions of failure indices in optimized angle-ply pipes (r_n = 75 mm, η = 0.25)

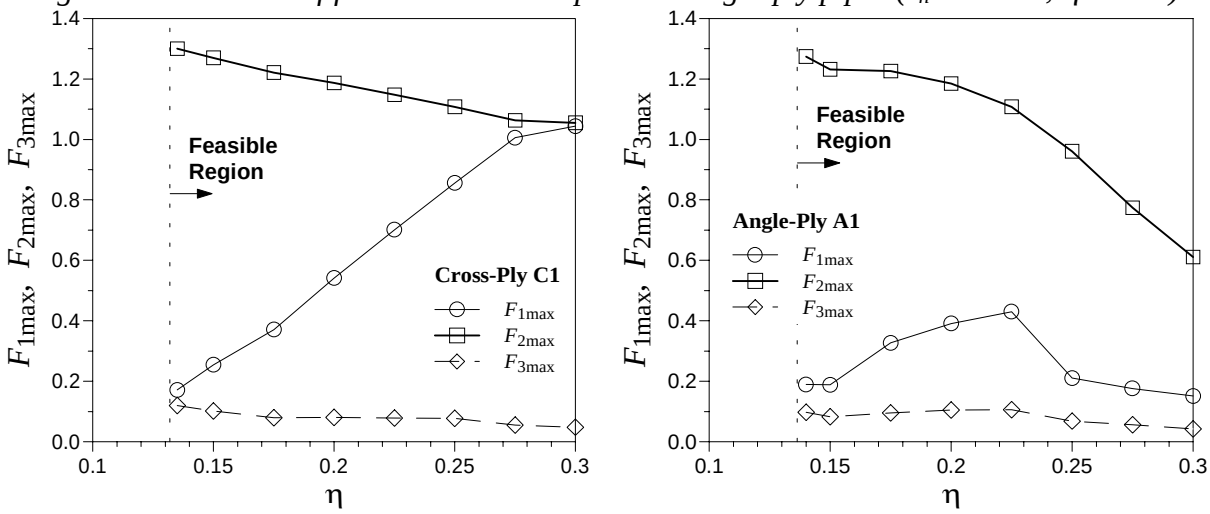

Fig. 7: Optimization results for CFRP pipes: effect of wall thickness (r_n = 75 mm)

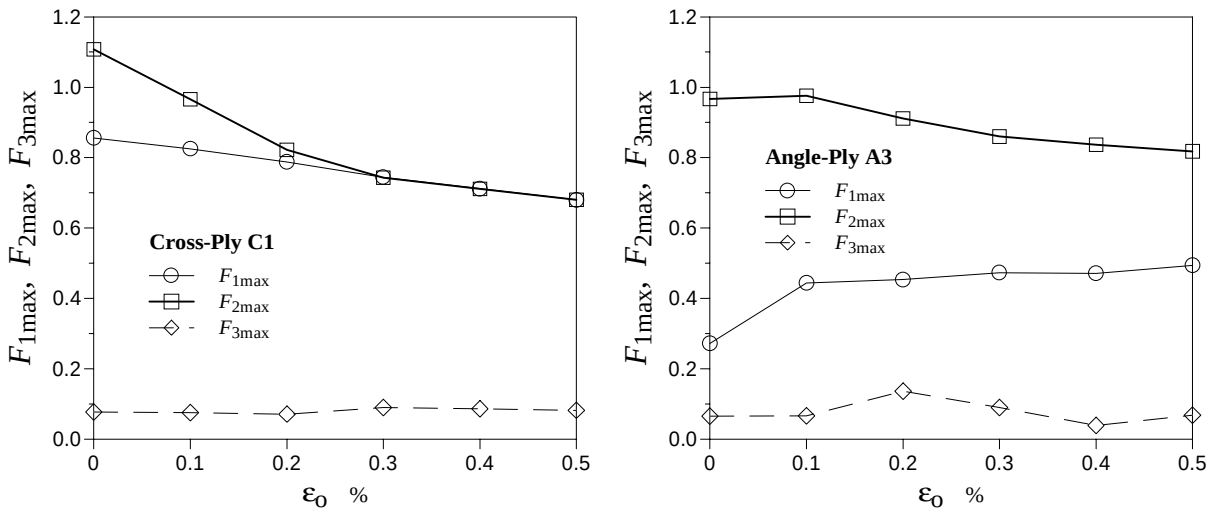

Fig. 8: Optimization results for CFRP pipes: effect of pre-tension (r_n = 75 mm, η = 0.25)

Effect of Wall Thickness

As shown in Fig. 7, the effect of the wall thickness h on the upper bounds of failure indices is investigated for the cross-ply and angle-ply pipes. The circular, square and diamond symbols correspond to F_{1max}, F_{2max} and F_{3max}, respectively. In the most calculations, the critical failure index is F_{2max}, indicating that matrix cracking is the primary mode of process-induced damages in the optimized CFRP pipes. As the wall thickness ratio η increases up to 0.3, F_{2max} decreases to 1.055 for C1 pipes and to 0.611 for A1 pipes. However, F_{1max} gradually increases to 1.044 for the cross-ply pipes. In addition, it must be noticed that the allowable lower limit, $I_{T\min}$ = 0.5 MN·m^2, of the torsional stiffness is imposed only in the angle-ply cases. Thus, it is concluded that the angle-ply lamination shows advantageous characteristics for thick-walled CFRP pipes.

Effect of Pre-Tension at Axial Plies

In order to reduce the risk of matrix cracking, it is efficient to mitigate the inherent anisotropic difference of the axial process-induced strain between the plies. One possible method may be the application of pre-tension at 0° plies in the axial direction. In Fig. 8, the effect of the axial pre-tension is illustrated for two types of CFRP pipes, where A3 pipe has a stacking sequence [$\pm\phi_1/\pm\phi_2/0/0/\pm\phi_4/\pm\phi_5$]. It is found that, as the pre-tension strain ε_o increases up to 0.5%, the critical index F_{2max} decreases to 0.680 for C1 pipe. The index F_{1max} for fiber breakage damage also decreases gradually, and becomes the same with F_{2max} when the pre-tension strain is equal to 0.3%. On the other hand, by applying the axial pre-tension at the 0° plies for angle-ply A3, the critical index F_{2max} can be reduced slightly.

CONCLUSIONS

In this study, an optimum design method for multi-layered thick-walled CFRP pipe is presented by minimizing the process-induced residual stresses in a strength-based sense. The analytical solutions of the residual stresses are based on quasi-static thermoelasticity and Hashin's failure criteria are used for the formation of the objective function. The global bending, transversely compressive and torsional stiffnesses are considered as structural constraints. The numerical results of optimization show that, in the case of cross-ply pipes,

the residual stresses can be reduced to a certain level by controlling ply thicknesses. Matrix cracking is the primary mode of damages in the thick-walled pipes because the transverse residual stress is considerable. For angle-ply pipes, by adjusting ply angles adequately, it is possible to further reduce the residual stresses with the large torsional stiffness. The effects of wall thickness and axial pre-tension on the optimum solutions are also investigated. In general, the process-induced residual stresses are superposed on the mechanically induced stresses in real operating environments. Therefore, it will be essential to design the composite pipes by considering the full interaction between the residual stresses and the mechanical stresses in detail.

REFERENCES

1. Padovan, J., "Thermoelasticity of Cylindrical Anisotropic Generally Laminated Cylinder", ASME *Journal of Applied Mechanics*, Vol. 43, 1976, pp. 124-130.

2. Hyer, M.W., Cooper, D.E. and Cohen, D., "Stresses and Deformations in Cross-Ply Composite Tubes Subjected to a Uniform Temperature Change", *Journal of Thermal Stresses*, Vol. 9, 1986, pp. 97-117.

3. Hyer, M.W. and Rousseau, C.Q., "Thermally Induced Stresses and Deformations in Angle-Ply Composite Tubes", *Journal of Composite Materials*, Vol. 21, 1987, pp. 454-480.

4. Tzeng, J.T. and Chien, L.S., "A Thermal/Mechanical Model of Axially Loaded Thick-Walled Composite Cylinders", *Composites Engineering*, Vol. 4, No. 2, 1994, pp. 219-232.

5. Sekine, H., Shin, E.S. and Viray, H.B., "Optimum Design of Filament-Wound Thick-Walled CFRP Pipes to Reduce Residual Stresses", *Proceedings of the Third International Conference on Materials Engineering for Resources*, Akita, Japan, 1998, pp. 126-134.

6. Adams, D.S., Bowles, D.E. and Herakovich, C.T., "Thermally induced transverse cracking in graphite-epoxy cross-ply laminates", *Journal of Reinforced Plastics & Composites*, Vol. 5, 1986, pp. 152-169.

7. Hashin, Z., "Failure Criteria for Unidirectional Fiber Composites", ASME *Journal of Applied Mechanics*, Vol. 47, 1980, pp. 329-334.